Direct Imaging of Exoplanets: Science and Techniques
Proceedings IAU Colloquium No. 200, 2005
C. Aime and F. Vakili

DOI: 00.0000/X000000000000000X

Pupil Replication: Implementation Aspects

Frank H. P. Spaan[1], Erwan Prot, Vincent Mourai, Alan H. Greenaway[1]

[1] School of Engineering and Physical Sciences, Heriot-Watt University, Edinburgh, United Kingdom.
email: F.Spaan@hw.ac.uk, A.H.Greenaway@hw.ac.uk

Abstract. In this paper we first introduce Pupil Replication. We then show simulation results for a pupil replicated classical coronagraph. Furthermore, we show experimental results as a proof of concept as well as a preliminary design for the replication optics.

Keywords. (stars:) planetary systems, instrumentation: high angular resolution, techniques: interferometric, techniques: miscellaneous, telescopes

1. Introduction

In a previous paper Greenaway et al (2005) we introduced the principle of Pupil Replication. This new optical technique decreases the diameter of the image of a star on, or very near to, the optical axis. Used as a supplementary system on a telescope with a coronagraph, an increase in the suppression of the star light is possible. The principle is shown in figure 1. A de-magnified image of the telescope entrance pupil is formed and several replications of the incoming wave at the entrance pupil are created optically and joined together side by side prior to being focused by an imaging system. For an on axis source this set up will act like a telescope with an increased diameter (see figure 1; dark grey lines), reducing the size of the original on-axis star image. For an off-axis source (light grey lines), like a planet to be detected, the width of the point spread function (PSF) is about the same as the width of the PSF without replication.

A currently important type of high dynamic range imaging is interferometric nulling. Applying pupil replication to such a nulling system does not lead to a straight forward improvement of the system. For another promising technique, pupil apodisation, including pupil replication in the system does lead to an increase in performance. Figure 2 shows an example where a 10^{10} times weaker planet becomes visible in most of the field beyond $1.6\lambda/D$. The extra peaks visible are due to chromatic smearing which stays within the diffraction limit of the telescope as shown in Greenaway et al (2005).

Both pupil apodisation and interferometric nulling lead to promising simulation results, but the requirements for building such systems are high. In this paper we look at a system that has lower requirements: a classical coronagraph with a hard-edged star-stop and Lyot-stop combined with pupil replication.

2. Pupil Replicated Classical Coronagraph

We look here at the possible implementation of Pupil Replication to a classical (Lyot) coronagraph. Since the (on-axis) star image size is reduced by pupil replication, an improvement in the star light suppression is expected. We simulated in two dimensions a

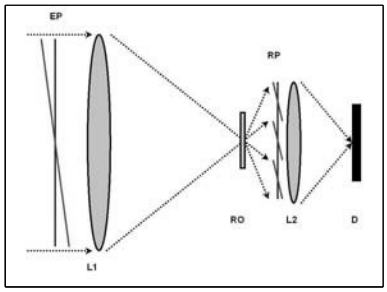

Figure 1. A schematic overview of the principle of Pupil Replication, shown here with 3 replications. The wave front, after passing through the entrance pupil (EP), is focused by the telescope (L1) and then divided equally in amplitude 3 ways using the replication optics (RO). Thus 3 replicated images of the entrance pupil are formed side by side in the replication plane (RP), each 1/3 of the intensity of the original pupil image. If the source is an axial point (dark grey lines) the replicated wave fronts form a continuous plane wave front. If the source is off axis (light grey lines), the replicated wave fronts form a disjointed wave front. The resulting wave front is passed through an imaging system (L2) and an image of the point object is formed through this lens on the detector (D).

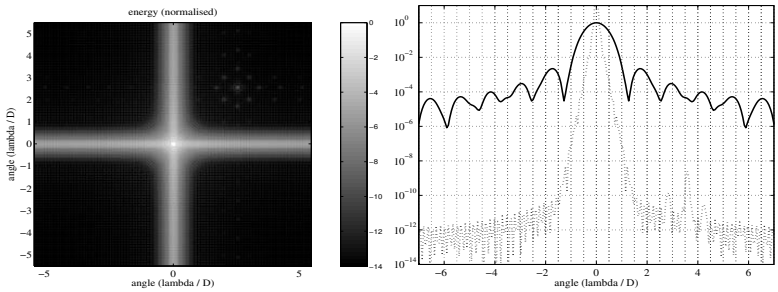

Figure 2. Simulation of a pupil apodisation system incorporating $8 * 8$ pupil replication. In the 2-D image (left) a planet (10^{-10}) is visible in the upper right corner. The right figure shows the diagonal crosssection. The system was simulated in the V-band and had an efficiency of 64%.

coronagraph with a hard edged image plane stop and Lyot stop, including Pupil Replication for a 3.5 meter telescope for two cases: a square input pupil in the V-band (which was simulated by 8 weighed wavelengths) and a hexagonal input pupil at $600nm$. None of this was optimised; the size of the Lyot stop was chosen to yield an efficiency of 50%. We first chose a square pupil and a replicated pupil existing of $8 * 8$ replicated input pupils; such a set up would be possible with a cascade of 6 of the replication optics described in section 3. The simulation results were obtained using a square star stop with a width of $2\lambda/D$ yielding an inner working angle of $1\lambda/D$. The PSF after the coronagraph for an on-axis source is shown in figure 3 (left). Cross sections through the PSF both for a system without (left) and with (right) pupil replication are shown in figure 4. For a square pupil the results in the different parts of the field are not the same: the diagonal cross section shows an attenuation that is overall much higher than the horizontal cross section. One can see on the left in figure 3 that most of the search area (over 90% in the image shown) has the characteristic of the diagonal cross section and can be used for search of high dynamic range objects.

For a hexagonal pupil we simulated a 7-fold replication system at one wavelength ($600nm$). As can be seen on the right in figure 3 the field is more homogeneous due to the more centro-symmetrical input pupil. The system we simulated had a hard edged

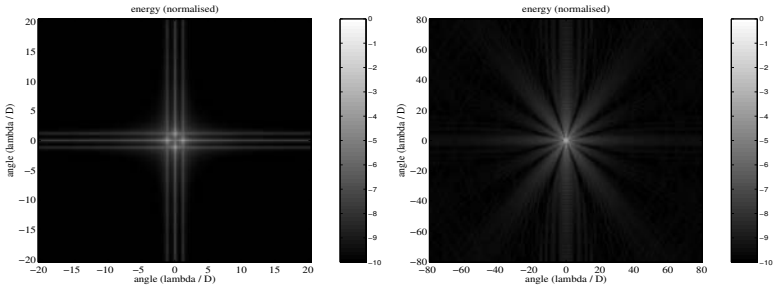

Figure 3. The PSF of the classical coronagraph with an on-axis source; using an $8*8$ replicated square pupil (left, simulation in the V-band) and using a 7-fold replicated hexagonal pupil (right, simulation at 600 nm).

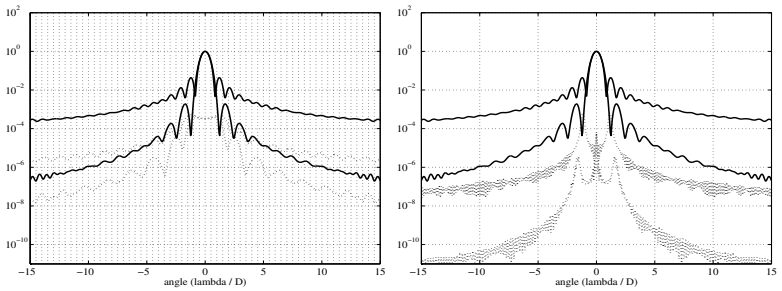

Figure 4. $8 * 8$ square pupil replication in the V-band. Cross sections through the PSF: left without and right with pupil replication. Solid and dotted lines: without and with star- and Lyot stop respectively. Both horizontal and diagonal cross sections are shown.

round star stop with a width of $2\lambda/D$, yielding a inner working angle of $1\lambda/D$ and a hard edged round Lyot stop. The horizontal and diagonal cross sections shown in figure 5 are now closer together. The absolute value of the attenuation is overall lower than in the example shown before because the number of replications is lower (7 instead of 64) and therefore the star image larger and the suppression of the star light less efficient.

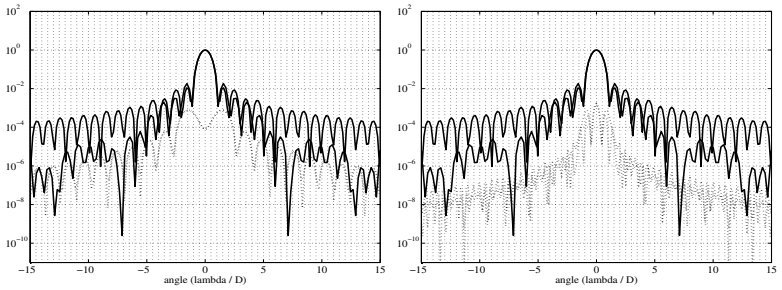

Figure 5. 7-fold hexagonal pupil replication at 600 nm. Cross sections through the PSF: left without and right with pupil replication. Solid and dotted lines: without and with star- and Lyot stop respectively. Both horizontal and diagonal cross sections are shown.

To make a first assessment of the influence of errors, we shifted one of the replicated hexagonal pupils (width 161 pixels) horizontally by 1 pixel (which is 0.6%) to the outside, leaving a gap along three hexagon sides. The result is shown in figure 6. We see the degradation in attenuation performance: the horizontal cross section does not get below 10^{-6}

within $15\lambda/D$. In Riaud et al. (2005) simulation results are given for a pupil apodised system including pupil replication which show a similar value: about 10^{-6} at $15\lambda/D$ and 0.5% rms shift error. Even though the performance is lower, the system seems to be not exceptionally sensitive to such an error taking into account that we have introduced a relatively high error that would be for a $16mm$ replication size a gap of 100μ width and $2.8mm$ length.

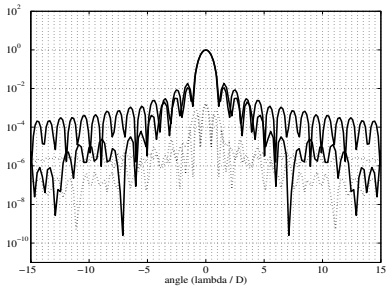

Figure 6. Results from a simulation of a classical coronagraph with pupil replication using a hexagonal pupil with 7 replications but with an error in the replication (see text).

3. Replication Optics

One of the parts of Pupil Replication that have not been assessed so far is the design for the optics that produce the replications of the pupil. A possible design for 2-fold replication of a rectangular input pupil is given here, see figure 7. The light entering from the top is split using a beam splitter. The two beams are then guided further using mirrors to be recombined. The last two mirrors are fixed to a translating element to change the beam separation. If we estimate the general efficiency of a mirror as 97%, the overall efficiency is about 88%. For a cascade of 6 replication optics to produce the 64 replications used in section 2 this would be 48%.Such optics can be put into solid glass (except for the last two mirrors). Furthermore, using the last two mirrors as shown, it is possible to eliminate a gap or overlap error. Finally, this system can be cascaded to obtain 2^n replicas.

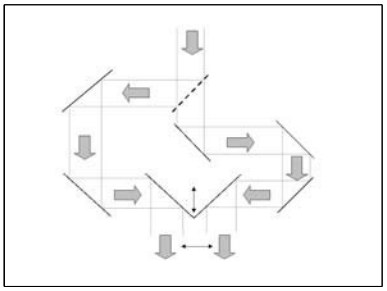

Figure 7. A design for the replication optics.

4. Experiment

An experiment was set up to test our theoretical model of pupil replication, see figure 8. Although pupil replication is meant to replicate the pupil in a telescope, we used for simplicity a laser beam instead of a telescope pupil to create the incoming wave front. The basic set up is that of a Mach-Zehnder interferometer, but instead of combining the two interferometer beams at the exit pupil so that they overlap, the beams were sheared with respect to each other. This way two disk shaped monochrome wave fronts are created at the exit pupil. These represent the replicated pupils in a telescope with pupil replication. In the experiment the two beams are then both imaged onto a detector through a single lens, as would be the case when applied to a telescope.

Figure 9 shows a typical set of images that were obtained. The top left picture shows

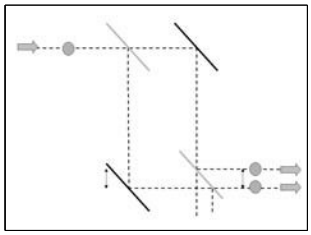

Figure 8. The experimental set up.

part of the beam at the exit pupil, the poor quality of the beam is visible; the optics used were of moderate quality. The interference in the right part of this picture is due to the other pupil replica. On the top right the cross section through this pupil image is shown. The second and third rows show the unreplicated PSF of each of the beams. The fourth row shows the decreased size of the PSF in the replicated system (shown later in more detail). The last image is saturated to show the side lobes of the replicated PSF.

We also simulated the experimental set up and then compared the simulation results

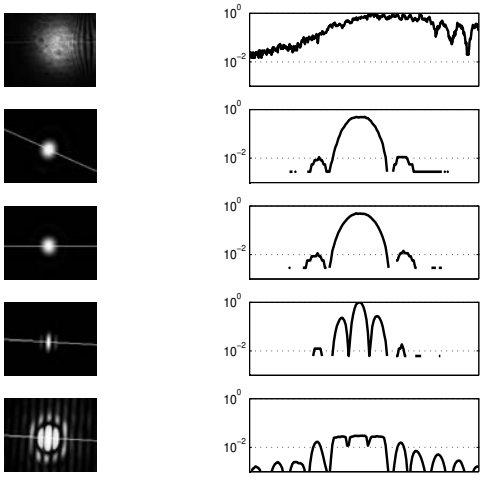

Figure 9. Experimental pictures (see text).

with the experimental results. We show here two cases at different values for the separation between the two pupil replicas (shear of the beams in the interferometer). In the figures only the cross sections through the two dimensional PSFs are shown.

In the left figure of figure 10 the separation is zero, that is the two discs are just touching each other. For the central and first order peaks the agreement between simulation and experiment is good; the third peaks come close to the lowest level of the CCD detector and the match here is less good; they are also subject to greater error.
On the right in figure 10 the separation is half the width of the beam, that is the two discs half overlap. Again, for the central and first order peaks the agreement between simulation and experiment is good, and for the third peaks less good. We also see that the central peak is now broader and the side lobes lower; this is because the separation is less than in the previous case.

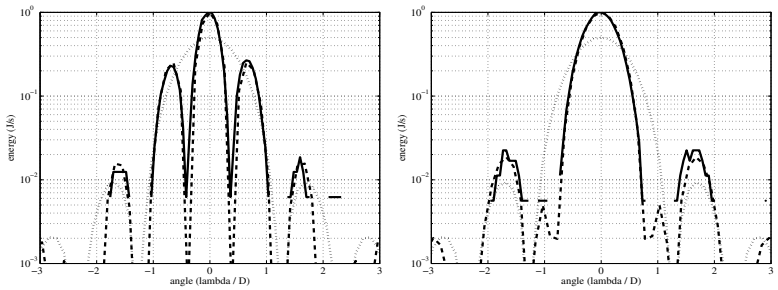

Figure 10. Left: Pupil replicas in contact (see figure 9): comparison with simulation results. Cross sections are shown of the simulated unreplicated PSF (dotted), of the simulated replicated PSF (dashed) and of the experimental replicated PSF (solid). Right: the same but now with half overlapping pupil replicas.

Finally some remarks about the experiment. The beam shape had a soft edge so that the experimental determination of the beam separation was difficult. In practise we adjusted the separation in the simulation to give a best fit of the PSFs. In our simulation we used a beam with a hard edge; a soft edged beam did not give better results. The saturated images we obtained gave more information on the higher order peaks, but a good fit with the simulation could not be obtained. The quality of the optics and other equipment used limited the results in this way. To get a better fit than shown, the optical defects would have to be taken into account in the simulation. Although imperfect, these experimental results give us confidence in our simulation.

Acknowledgements

We would like to acknowledge the funding by PPARC.

References

Greenaway, A. H., Spaan, F. H. P. & Mourai, V. 2005, *Astrophysical Journal Letters*, 618-2, L165.

Riaud, P., Mawet, D. & Absil, O. 2005, *Astrophysical Journal Letters*, 628-2, L81.

Discussion

We have shown simulation results for a pupil replicated classical coronagraph, which indicated the increase in performance when using a pupil replicated system. We also showed an experimental proof of principle and a design for the replication optics. These results overall bring actual implementation of pupil replication in a coronagraphic system a step nearer.